Electronic Supplementary Material (ESI) for Dalton Transactions.

Supporting Information

An Experimental and Theoretical Study of the Coordination and Donor Properties of Tris-2-pyridyl-phosphine Ligands

Schirin Hanf,[a,c] Annie L. Colebatch,[a,b] Philipp Stehr,[c] Raúl García-Rodríguez,[d] Evamarie Hey-Hawkins,*[c]
Dominic S. Wright*[a]

[a]Dr. S. Hanf, Dr. A. L. Colebatch, Prof. Dr. D. S. Wright, Chemistry Department, University of Cambridge, Lensfield Road, CB2 1EW, Cambridge, UK. E-mail: dsw1000@cam.ac.uk

[b]Dr. A. L. Colebatch, Research School of Chemistry, Australian National University, Canberra, ACT 2601, Australia.

[c]Dr. S. Hanf, P. Stehr, Prof. Dr. E. Hey-Hawkins, Institute of Inorganic Chemistry, Faculty of Chemistry and Mineralogy, Leipzig University, Johannisallee 29, 04103 Leipzig, Germany. E-mail: hey@uni-leipzig.de

[d]Dr. R. García-Rodríguez, GIR MIOMeT-IU Cinquima-Química Inorgánica Facultad de Ciencias, Universidad de Valladolid, Campus Miguel, Delibes, 47011 Valladolid, Spain.

Content

1.) Syntheses of complexes 14 – 16

Synthesis of [W(CO)$_4${P(2-py)$_3$-κ^2*N,N'*}] (13) and *cis*-[W(CO)$_4${P(2-py)$_3$-κ^1*P* }$_2$] (14)

A mixture of P(2-py)$_3$ (50 mg, 0.19 mmol) and 5 ml of acetonitrile was treated with [W(CO)$_5$(MeCN)] (0.30 ml, 0.19 mmol). The reaction mixture was stirred for 6 days at room temperature. The resulting red brown solution was filtered, and the solvent was removed *in vacuo*. A mixture of small black crystals and colourless crystals (of **13**·DCM and **14**, respectively) were grown from layering a DCM solution with *n*-hexane at –25 °C for 6 days. Compounds **13**·DCM and **14** could not be characterised completely due to their inseparability. ^{31}P{^{1}H} NMR (CDCl$_3$, 161.99 MHz), δ [ppm] = 33.5 (s, $^1J_{\mathrm{PW}}$ = 118.3 Hz, **14**), –8.2 (s, **13**).

Synthesis of [Mo(CO)$_3${P(6-Me-2-py)$_3$-κ^3*N,N',N''*}] (15)

A mixture of P(6-Me-2-py)$_3$ (51 mg, 0.17 mmol) and [Mo(CO)$_3$(η^6-C$_7$H$_8$)] (0.46 mg, 0.17 mmol) in 5 ml of acetonitrile was stirred for 20 hours at room temperature. The resulting orange solution was filtered and added to 15 ml *n*-hexane to produce an orange oil. The solution was decanted and the oil dried under vacuum. A small amount of red crystals was grown from layering a THF solution with toluene at room temperature. Compound **15** could not be characterised completely due to its inseparability from other products. ^{31}P{^{1}H} NMR (CDCl$_3$, 162.02 MHz), δ [ppm] = 0.7 (s).

Synthesis of [Mo$_2$(CO)$_6${P(6-Me-2-py)$_3$-μ^2:*κ^{1}P;κ^{3}N,N',C,C'*}{P(6-Me-2-py)$_3$-κ^2*P,N*}] (16)

A solution of [Mo(CO)$_6$] (0.17 g, 0.66 mmol) in 10 ml of acetonitrile was heated at reflux for 6 hours then allowed to cool. Ligand **2** (0.20 g, 0.65 mmol) in 10 ml of acetonitrile was added to the yellow solution. The resulting red-brown suspension was heated at reflux for 17 hours. The precipitate was filtered off and the solvent was removed from the filtrate under vacuum. Red crystals (accompanied by brown precipitate) were grown from layering a DCM solution with *n*-hexane. Compound **16**·DCM could not be characterised completely due to its inseparability from other products. ^{31}P{^{1}H} NMR (C$_6$D$_6$, 162.02 MHz), δ [ppm] = 68.8 (d, J_{PP} = 23 Hz), 4.2 (d, J_{PP} = 23 Hz).

2.) Selected NMR spectra

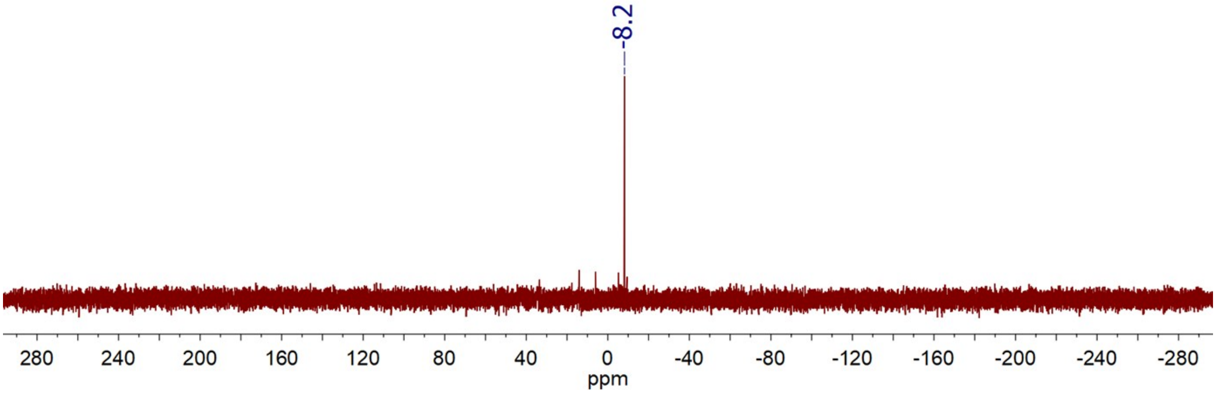

Figure S1: $^{31}P\{^1H\}$ NMR (298 K, $CDCl_3$, 161.99 MHz) spectrum of $[W(CO)_4\{P(2\text{-py})_3\text{-}\kappa^2 N,N'\}]$ (**13**).

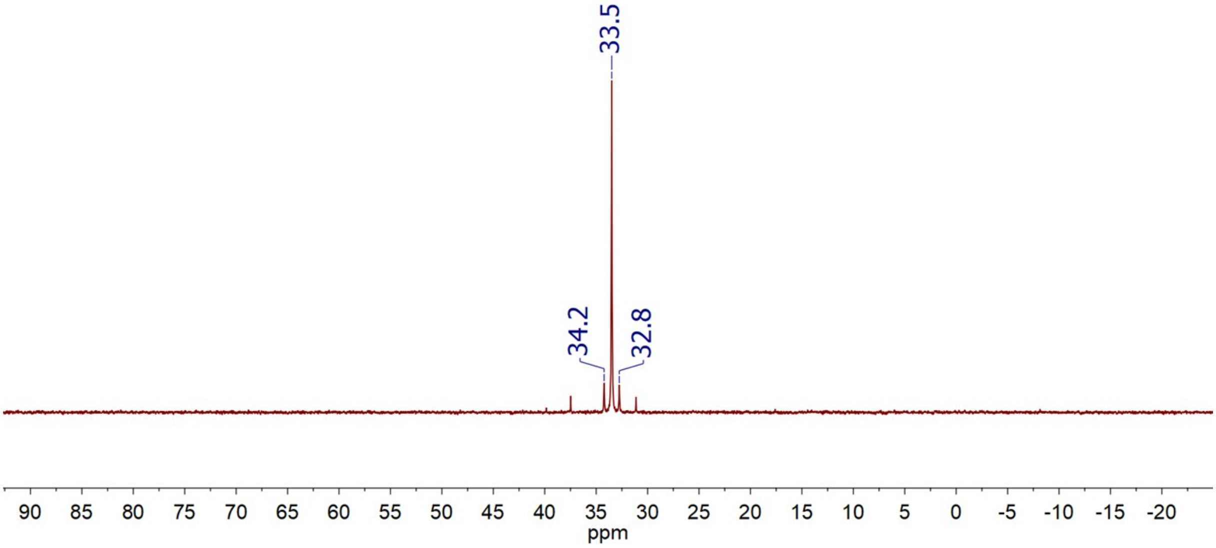

Figure S2: $^{31}P\{^1H\}$ NMR (298 K, $CDCl_3$, 161.99 MHz) spectrum of *cis*-$[W(CO)_4\{P(2\text{-py})_3\text{-}\kappa^1 P\}_2]$ (**14**).

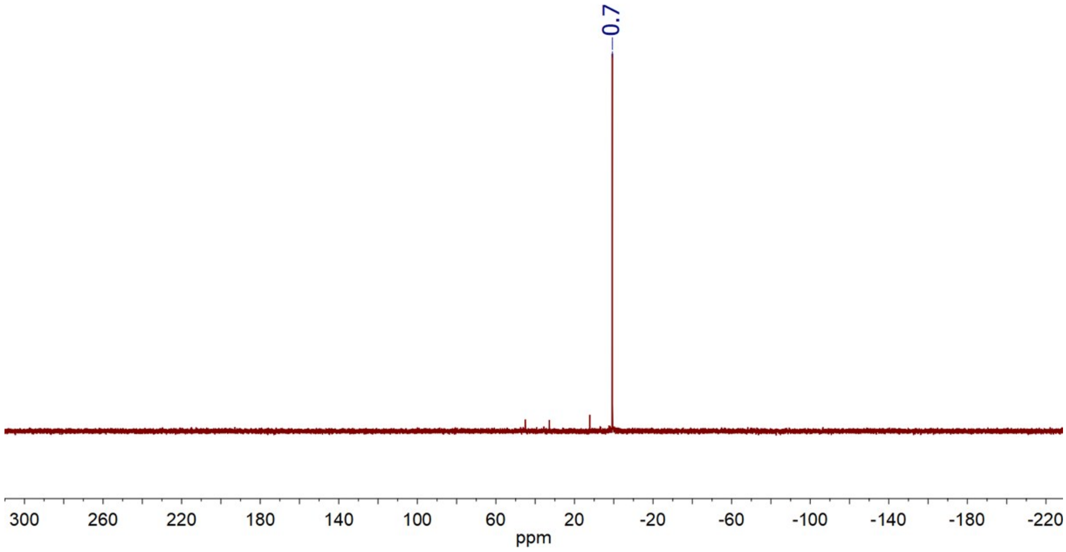

Figure S3: $^{31}P\{^1H\}$ NMR (298 K, $CDCl_3$, 162.02 MHz) spectrum of $[Mo(CO)_3\{P(6\text{-Me-2-py})_3\text{-}\kappa^3 N,N',N''\}]$ (**15**).

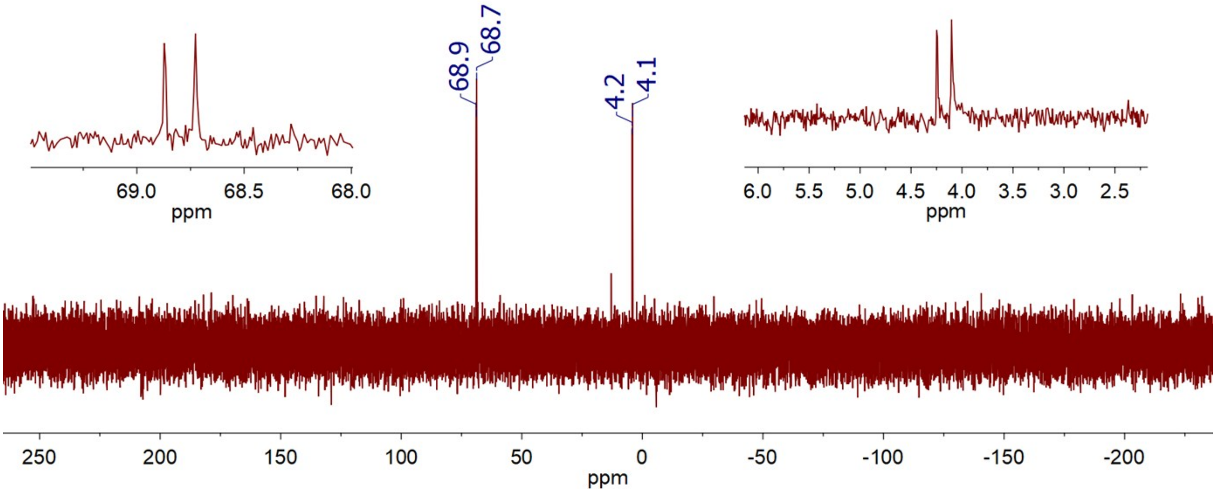

Figure S4: $^{31}P\{^1H\}$ NMR (298 K, CD_6D_6, 162.02 MHz) spectrum of $[Mo_2(CO)_6\{P(6\text{-}Me\text{-}2\text{-}py)_3\text{-}\mu^2{:}\kappa^1P;\kappa^3N,N',C,C'\}\{P(6\text{-}Me\text{-}2\text{-}py)_3\text{-}\kappa^2P,N\}]$ (**16**)

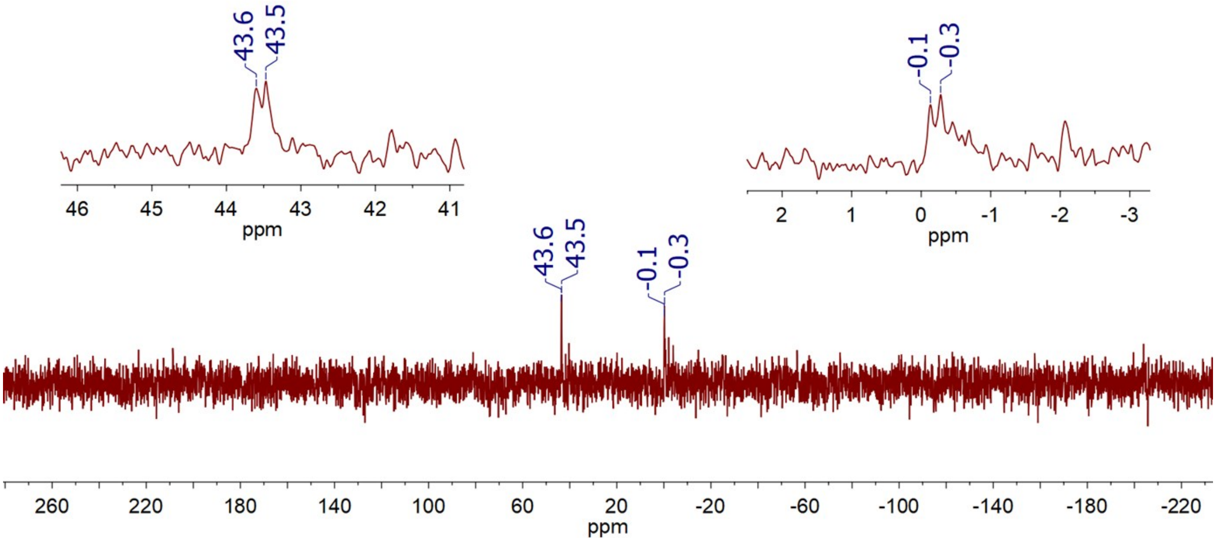

Figure S5: $^{31}P\{^1H\}$ NMR (298 K, CD_3CN, 162.02 MHz) spectrum of $[Mo_2(CO)_6\{P(6\text{-}Me\text{-}2\text{-}py)_3\text{-}\mu^2{:}\kappa^1P;\kappa^3N,N',C,C'\}\{P(6\text{-}Me\text{-}2\text{-}py)_3\text{-}\kappa^2P,N\}]$ (**16**). The solubility of **16** in CD_3CN was very low and the line broadening has been adjusted.

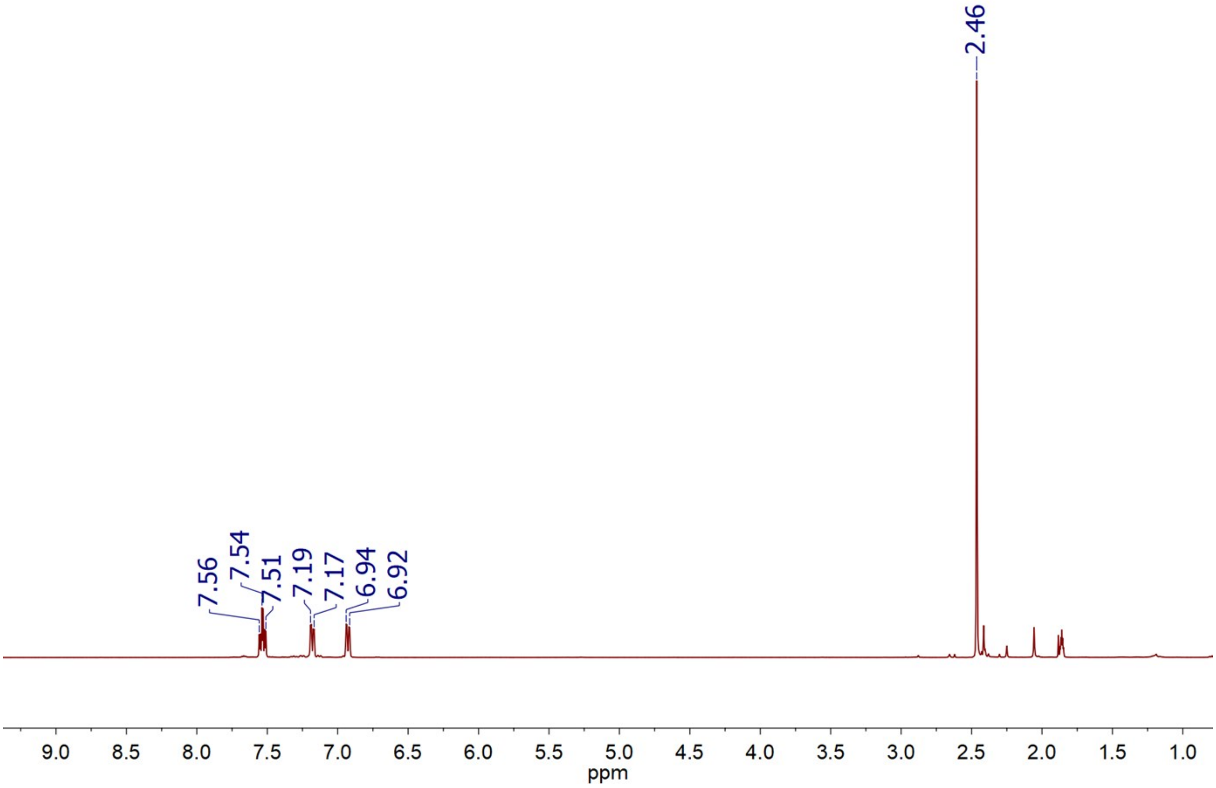

Figure S6: ^{1}H NMR (298 K, CD_3CN, 400.16 MHz) spectrum of $[Mo(CO)_5\{P(6\text{-}Me\text{-}2\text{-}py)_3\text{-}\kappa^1P\}]$ (**17**).

Note: Small amounts of impurities in the aliphatic and aromatic region of the ^{1}H NMR spectrum were observed, since compound **17** readily oxidises or hydrolyses in the NMR tube after prolonged storage.

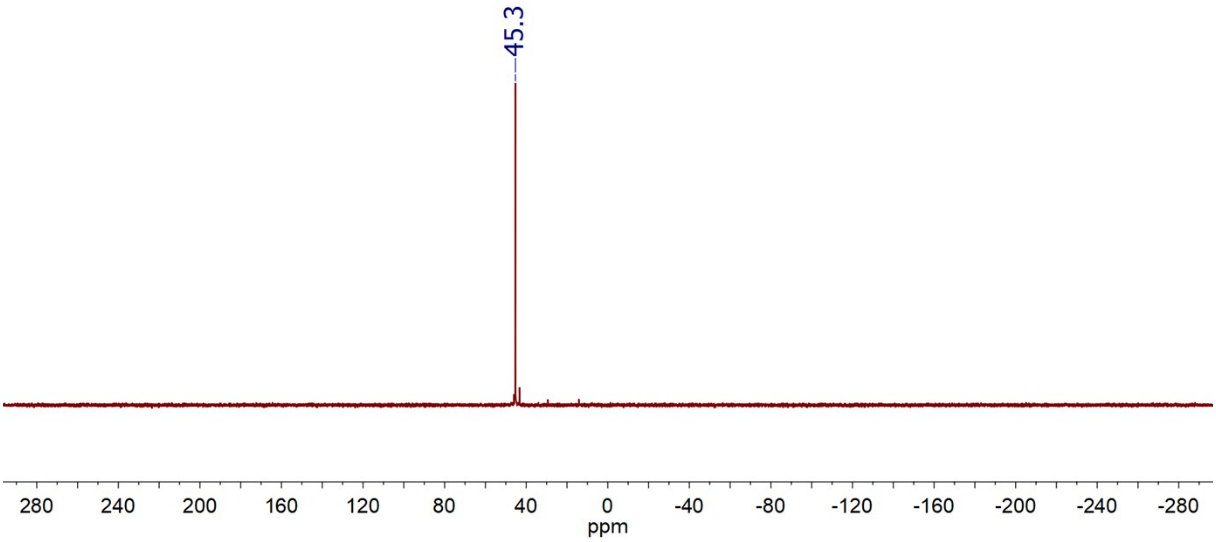

Figure S7: $^{31}P\{^1H\}$ NMR (298 K, CD_3CN, 161.99 MHz) spectrum of $[Mo(CO)_5\{P(6\text{-}Me\text{-}2\text{-}py)_3\text{-}\kappa^1P\}]$ (**17**).

Note: A small amount of an impurity at 43.3 ppm (6 %) was observed in the $^{31}P\{^1H\}$ NMR spectrum, since compound **17** readily oxidises or hydrolyses in the NMR tube after prolonged storage.

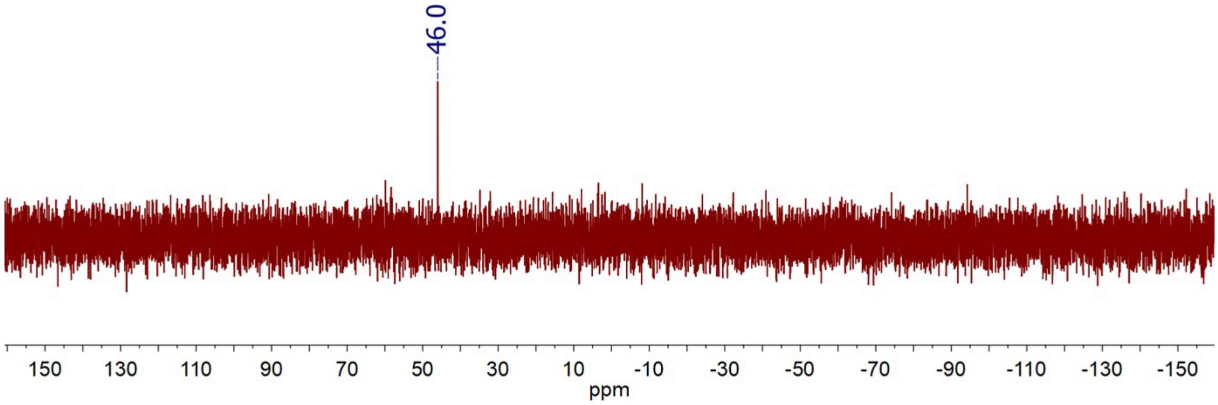

Figure S8: *In-situ* ^{31}P{^{1}H} NMR (298 K, CDCl$_3$, 161.99 MHz) spectrum of the reaction of [Me(CO)$_5$(MeCN)] with P(6-Me-2-py)$_3$. The reaction was carried out in MeCN, for the NMR spectrum 0.1 mL of CDCl$_3$ were added.

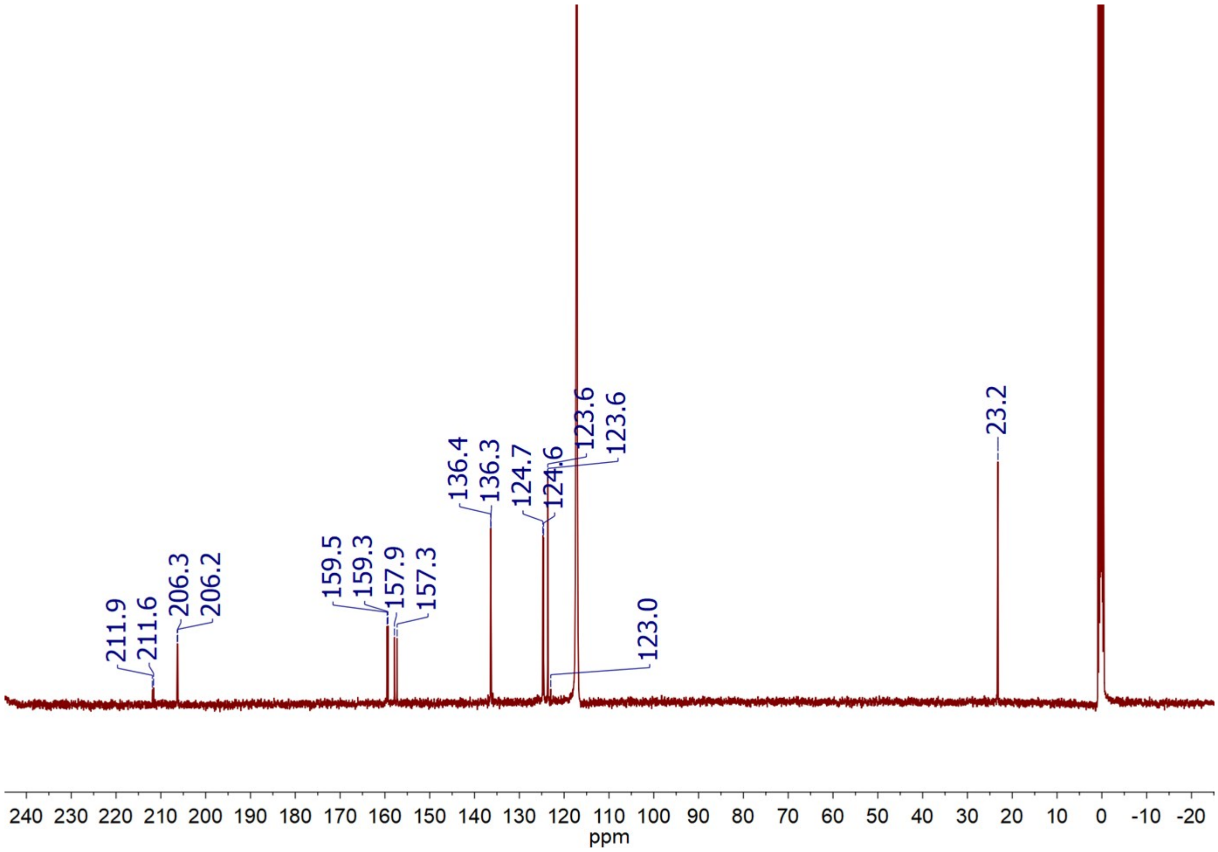

Figure S9: ^{13}C{^{1}H} NMR (298 K, CD$_3$CN, 100.63 MHz) spectrum of [Mo(CO)$_5${P(6-Me-2-py)$_3$-κ^1P}] (**17**).

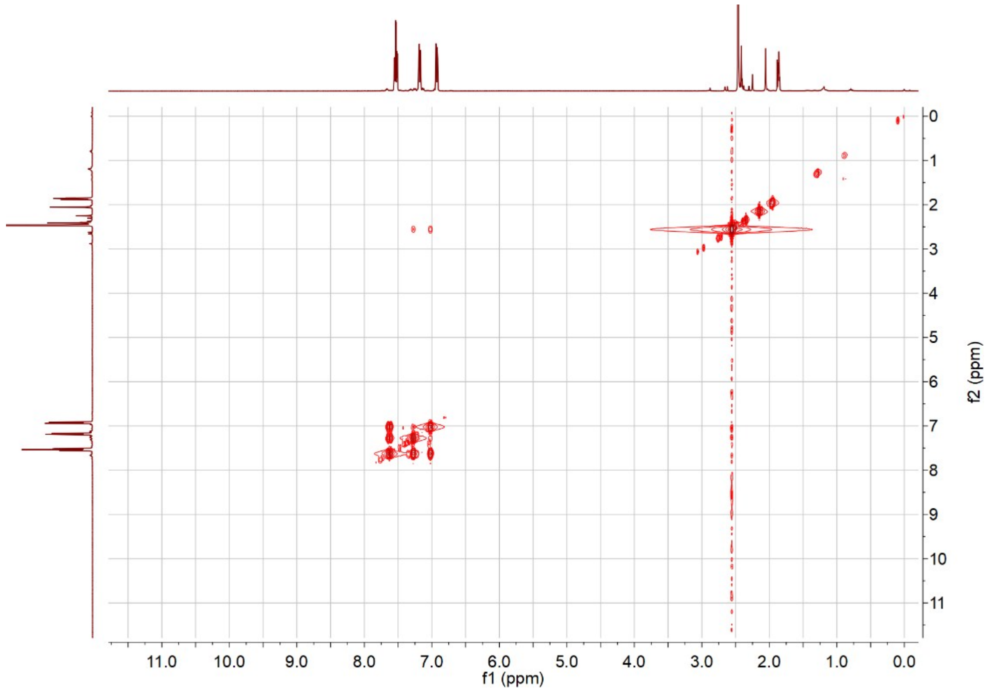

Figure S10: ^{1}H-^{1}H COSY NMR (298 K, CD_3CN, 400.16 MHz) spectrum of [Mo(CO)$_5${P(6-Me-2-py)$_3$-κ^1P}] (**17**).

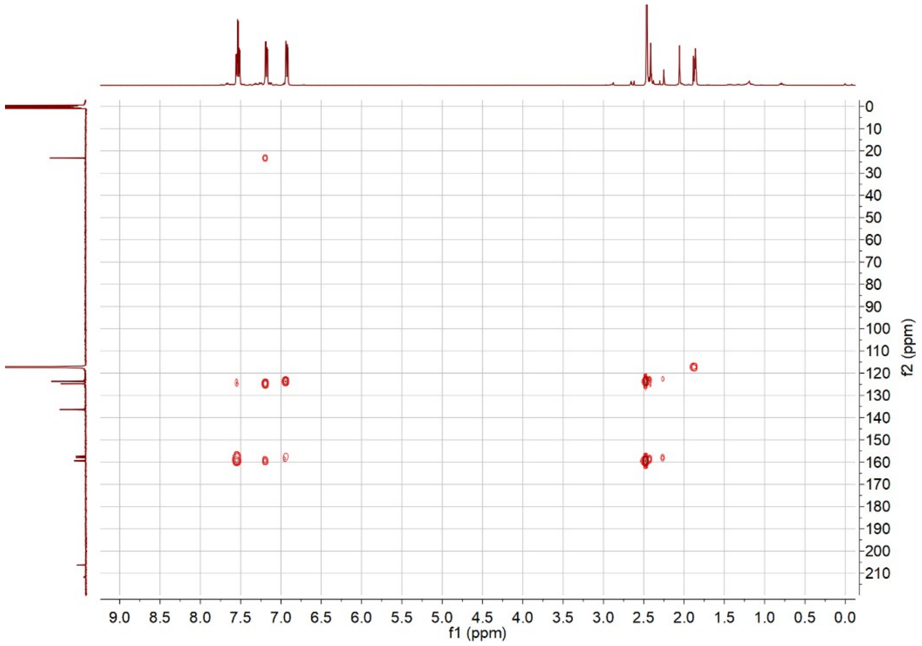

Figure S11: ^{1}H-^{13}C HMBC NMR (298 K, CD_3CN, 400.16 MHz, 100.63 MHz) spectrum of [Mo(CO)$_5${P(6-Me-2-py)$_3$-κ^1P}] (**17**).

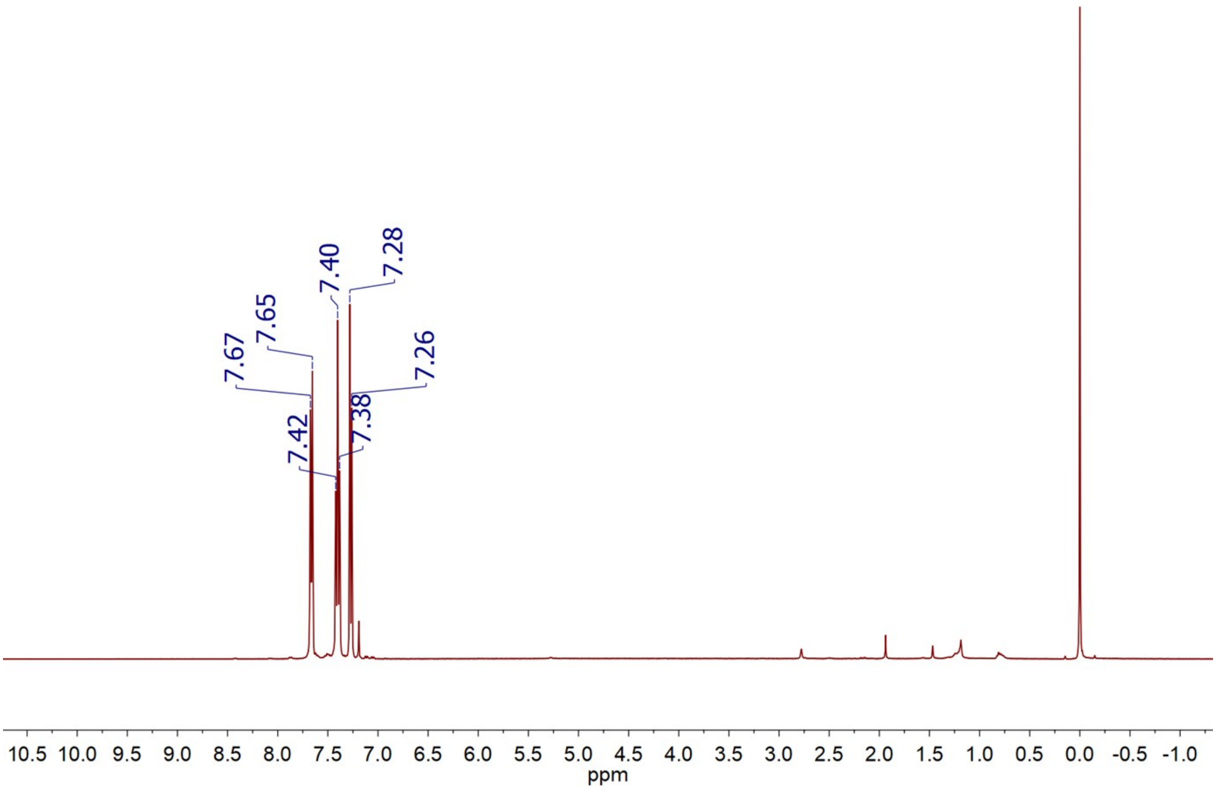

Figure S12: ^{1}H NMR (298 K, $CDCl_3$, 400.16 MHz) spectrum of *cis*-[Mo(CO)$_4${P(6-Br-2-py)$_3$-κ^1*P*}$_2$] (**19**).

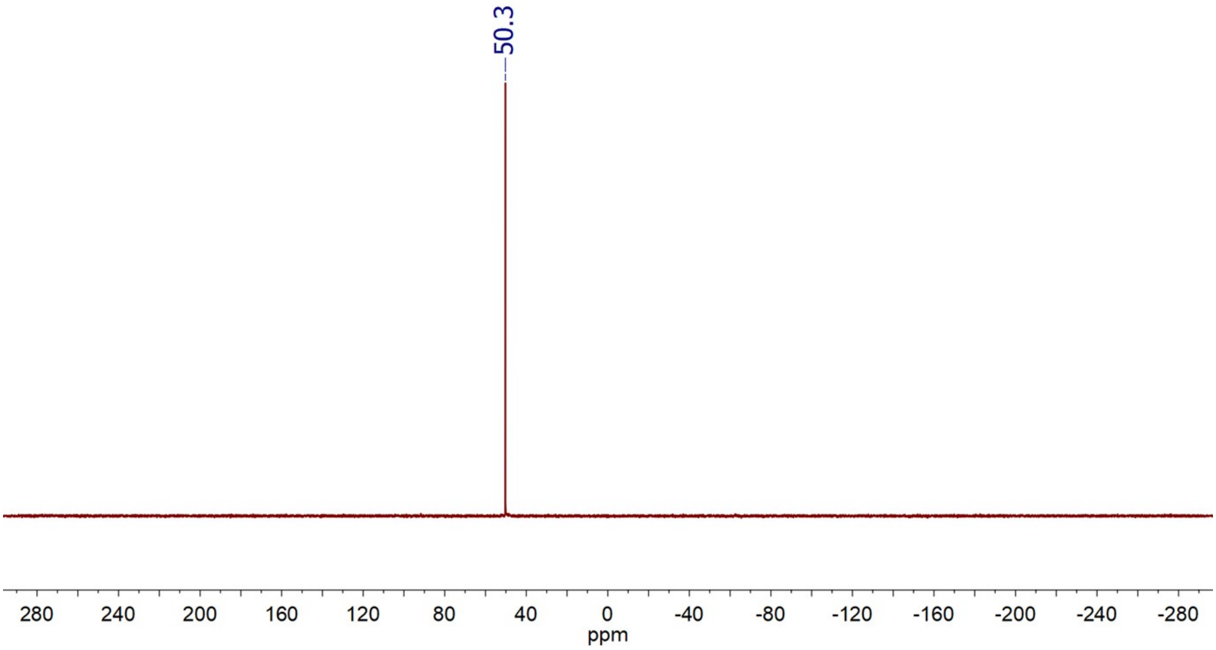

Figure S13: ^{31}P{^{1}H} NMR (298 K, $CDCl_3$, 161.99 MHz) spectrum of *cis*-[Mo(CO)$_4${P(6-Br-2-py)$_3$-κ^1*P*}$_2$] (**19**).

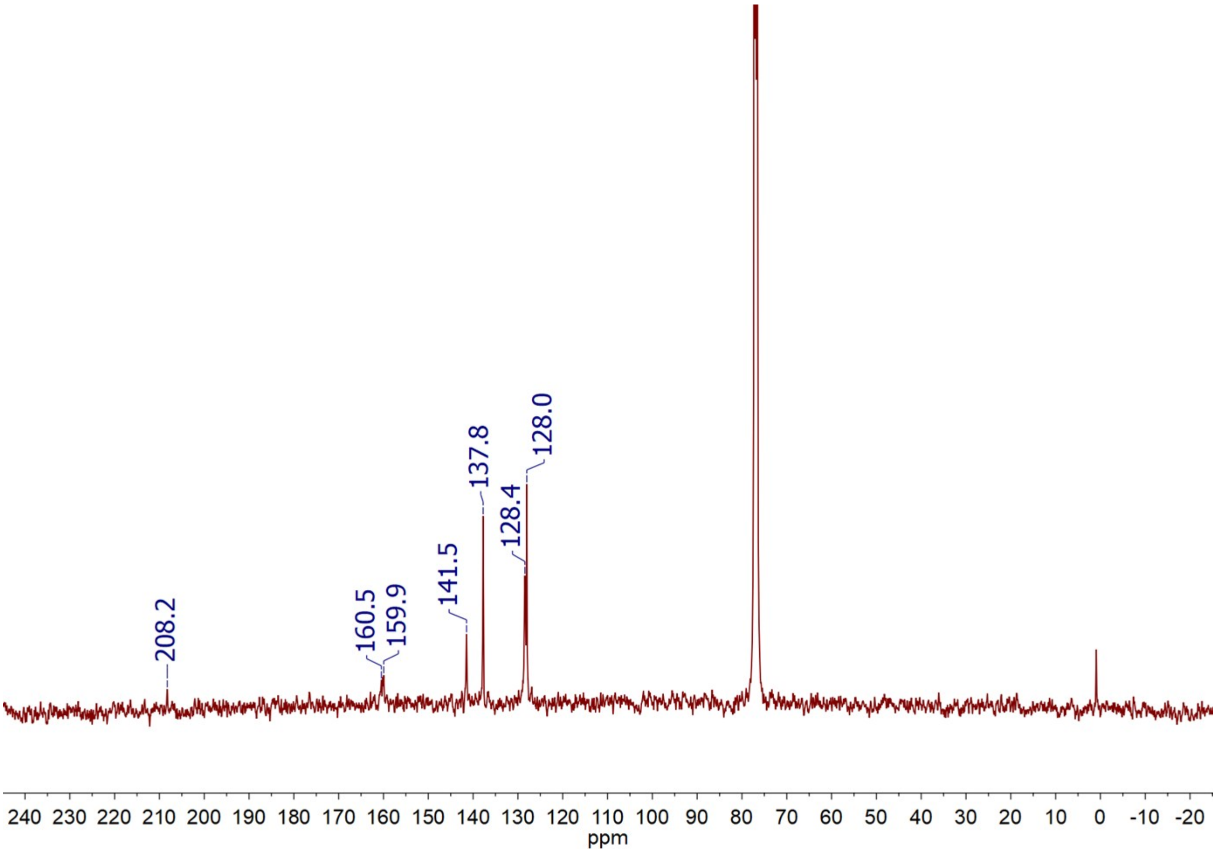

Figure S14: $^{13}C\{^1H\}$ NMR (298 K, $CDCl_3$, 100.63 MHz) spectrum of *cis*-[Mo(CO)$_4${P(6-Br-2-py)$_3$-κ^1*P*}$_2$] (**19**).

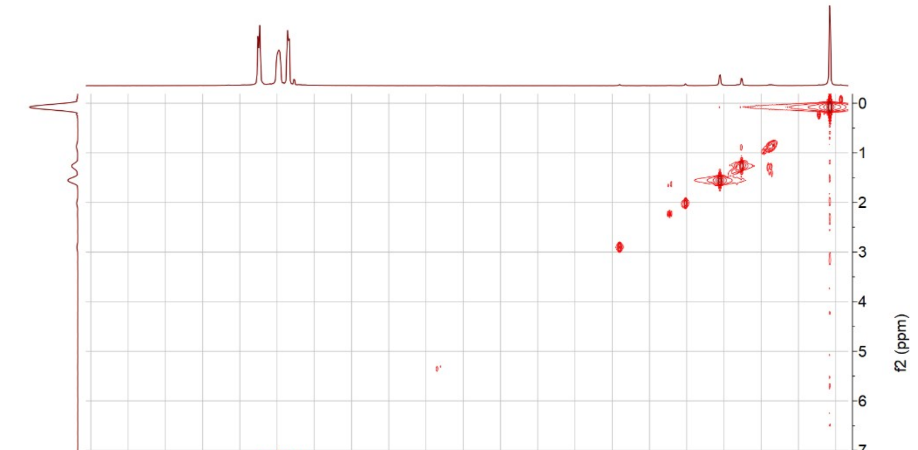

Figure S15: ^1H-^1H COSY NMR (298 K, $CDCl_3$, 400.16 MHz) spectrum of *cis*-[Mo(CO)$_4${P(6-Br-2-py)$_3$-κ^1*P*}$_2$] (**19**).

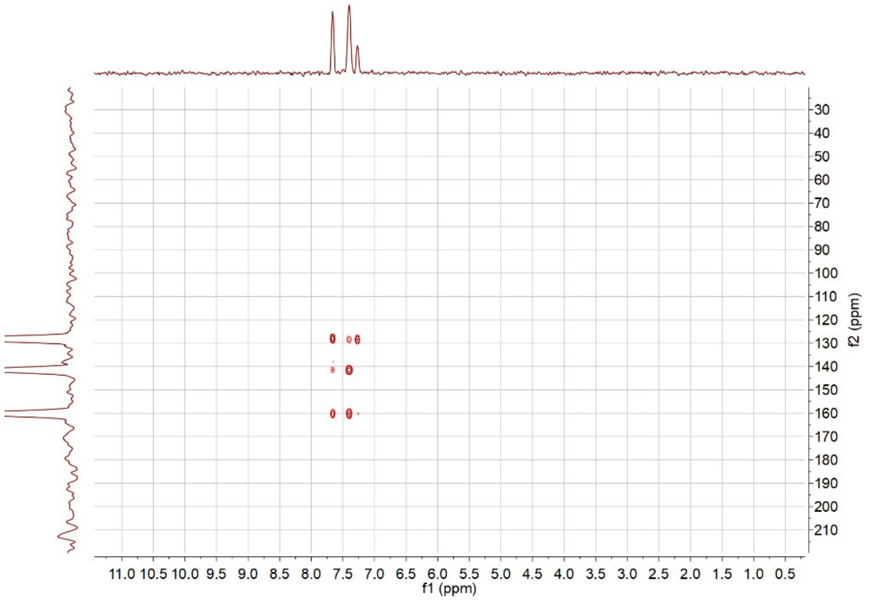

Figure S16: ^{1}H-^{13}C HMBC NMR (298 K, $CDCl_3$, 400.16 MHz, 100.63 MHz) spectrum of *cis*-[Mo(CO)$_4${P(6-Br-2-py)$_3$-κ^1*P*}$_2$] (**19**).

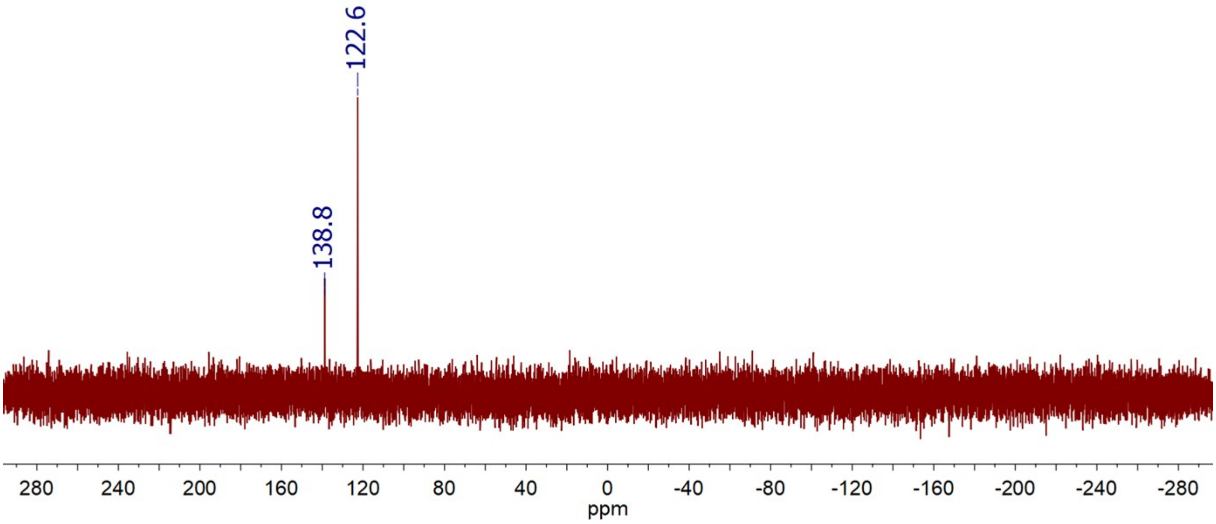

Figure S17: $^{31}P\{^{1}H\}$ NMR (298 K, C_6D_6, 161.99 MHz) spectrum the reaction mixture of $(Et_2N)_2P(2\text{-py})$ (**7**) and [Mo(CO)$_5$(MeCN)] in MeCN. For the recording of the NMR spectrum 0.1 mL C_6D_6 were added.

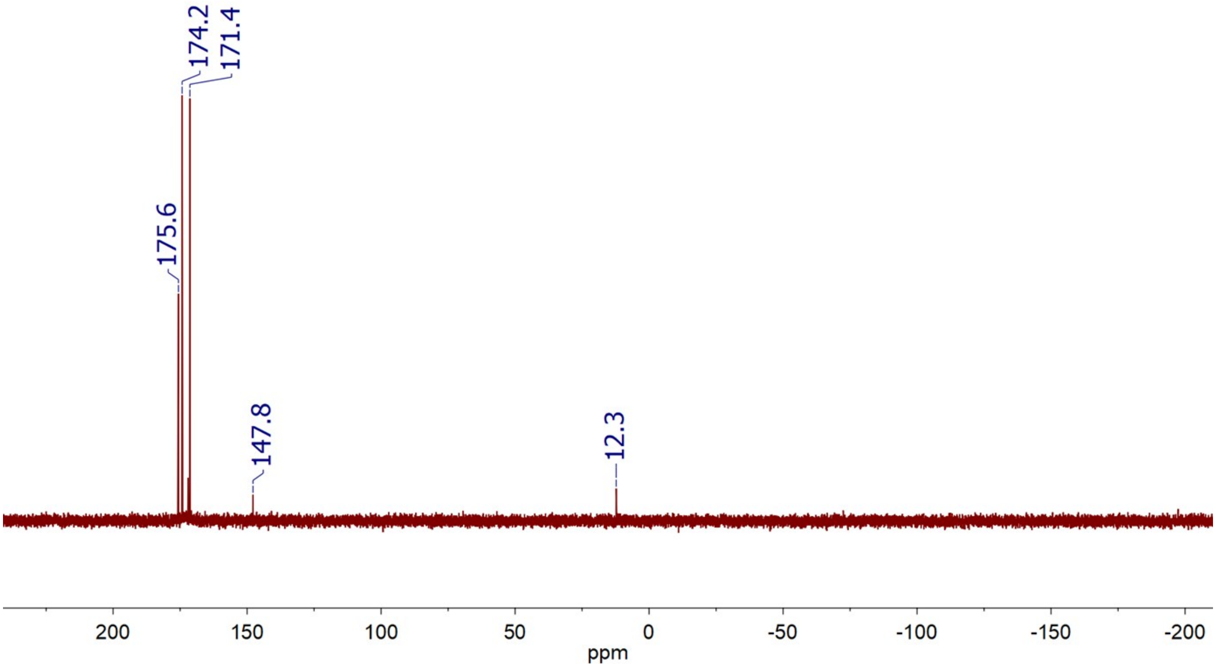

Figure S18: $^{31}P\{^{1}H\}$ NMR (298 K, C_6D_6, 161.99 MHz) spectrum the reaction mixture of $(MeO)_2P(2\text{-}py)$ (**10**) and $[Mo(CO)_5(MeCN)]$ in MeCN. For the recording of the NMR spectrum 0.1 mL C_6D_6 were added.

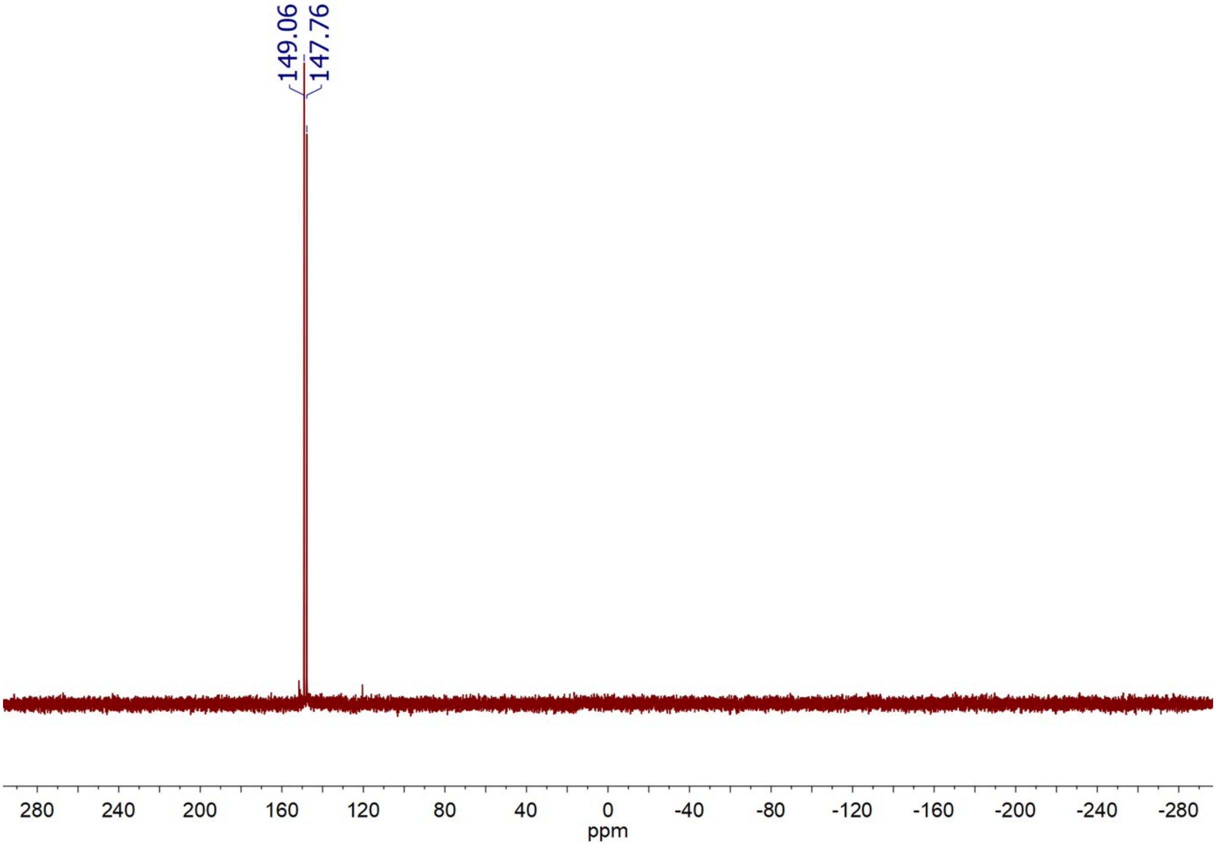

Figure S19: $^{31}P\{^{1}H\}$ NMR (298 K, C_6D_6, 161.99 MHz) spectrum the reaction mixture of $(Et_2N)(PhO)P(2\text{-}py)$ (**12**) and $[Mo(CO)_5(MeCN)]$ in MeCN. For the recording of the NMR spectrum 0.1 mL C_6D_6 were added.

3.) IR spectra

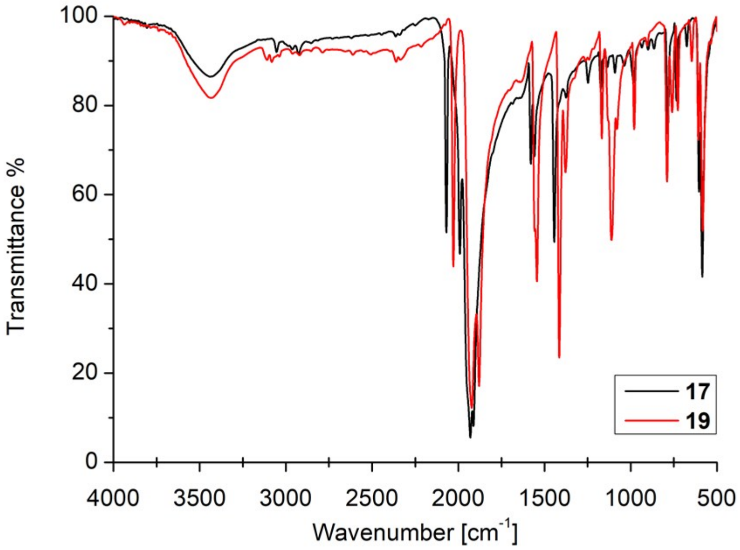

Figure S20: IR spectra of complexes **17** and **19**, measured as KBr pellets in the solid-state. The bands at 3500 cm^{-1} are due to water residues in the KBr.

4.) HR ESI mass spectrometry

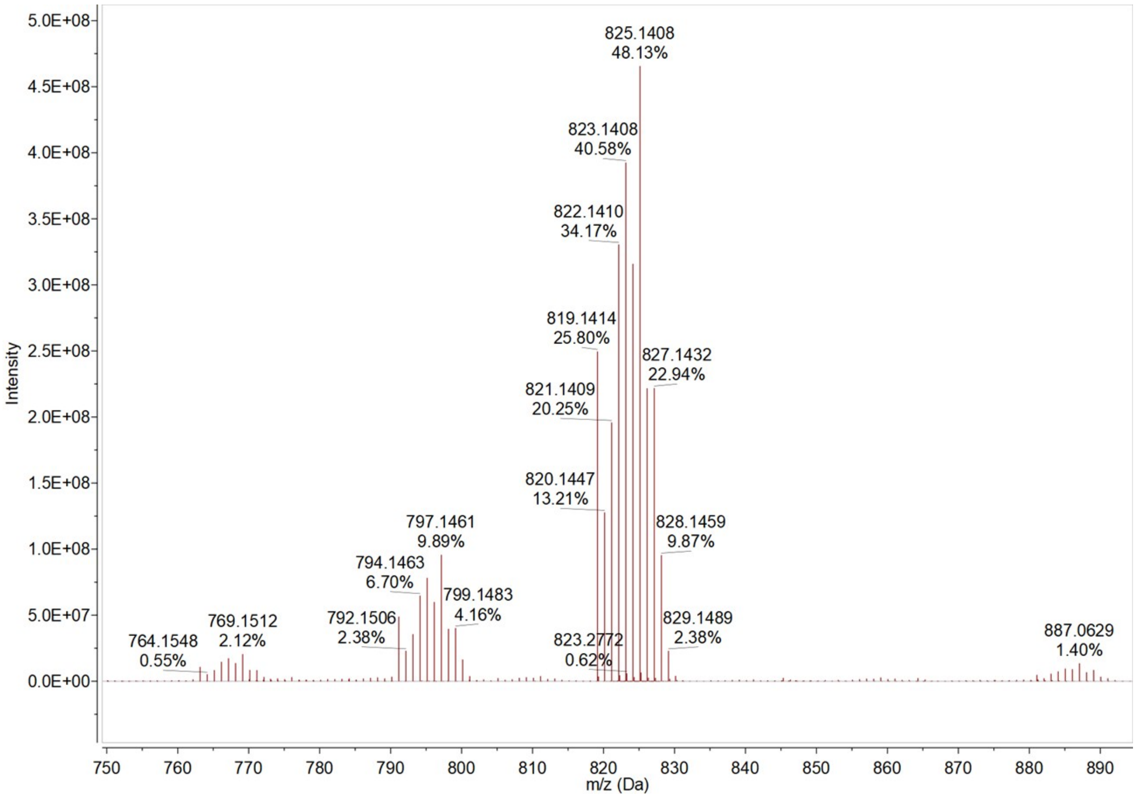

Figure S21: Extract of the HR ESI MS spectrum of [Mo(CO)$_5${P(6-Me-2-py)$_3$-κ^1*P*}] (**17**).

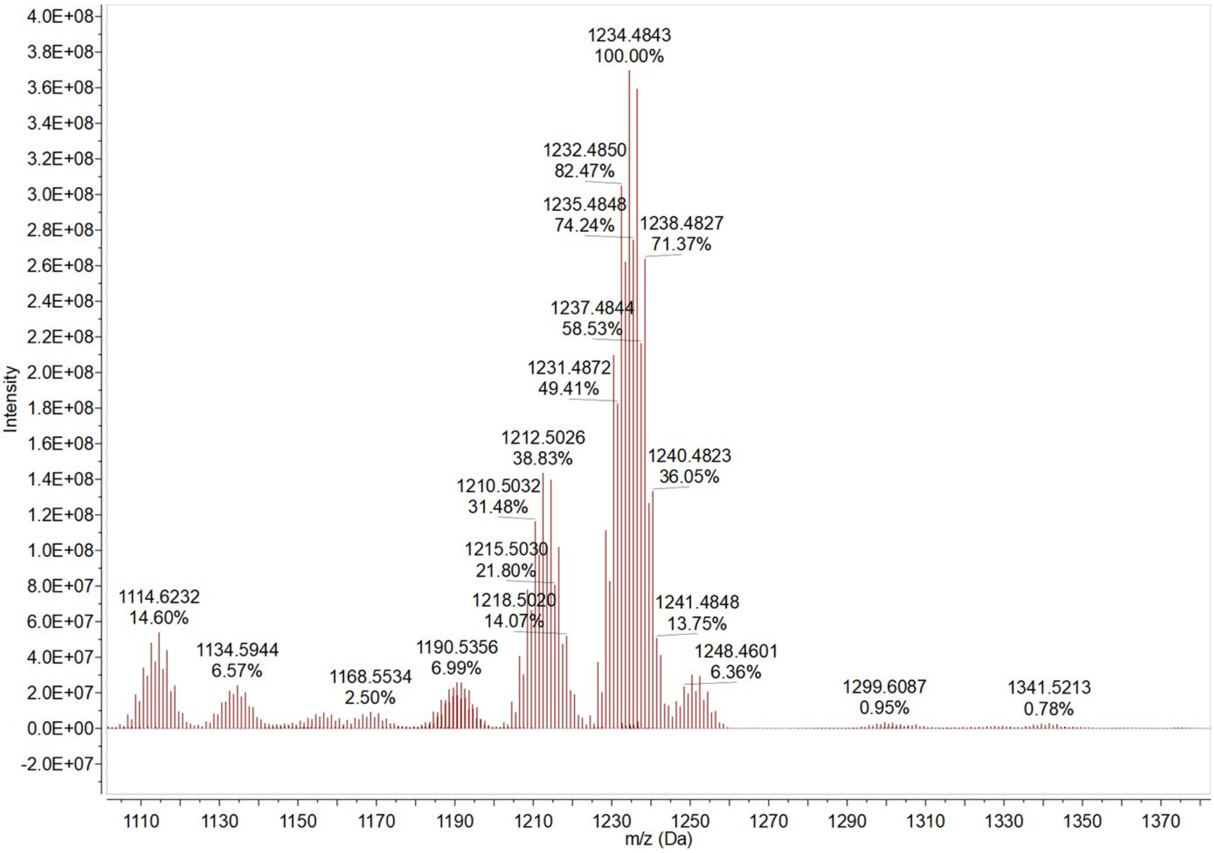

Figure S22: Extract of the HR ESI MS spectrum of [Mo(CO)$_4${P(6-Br-2-py)$_3$-κ^1*P*}$_2$] (**19**).

5.) Single-crystal X-ray crystallography

Table S1: Crystallographic parameters of the complexes **13** – **17**.

	13·DCM	**14**	**15**	**16**·DCM
CCDC number	1983665	1983667	1983663	1983662
Chemical formula	$C_{20}H_{14}N_3PO_4Cl_2W$	$C_{34}H_{24}N_6P_2O_4W$	$C_{21}H_{18}MoN_3O_3P$	$C_{43}H_{38}Cl_2Mo_2N_6O_6P_2$
Formula mass	646.06	826.38	487.31	1059.54
Crystal system	triclinic	orthorhombic	monoclinic	monoclinic
a/Å	10.5568(3)	17.0942(2)	9.3290(3)	14.6757(6)
b/Å	14.7613(5)	10.2626(1)	14.1222(5)	15.6115(6)
c/Å	15.4570(4)	17.9547(2)	14.9039(6)	21.3053(8)
α/°	105.255(3)	90	90	90
β/°	108.189(3)	90	92.6570(13)	109.233(2)
γ/°	92.397(3)	90	90	90
Unit cell volume/Å^3	2187.4(1)	3149.81(6)	1961.42(12)	4608.8(3)
Temperature/K	130	130	180	180
Space group	$P\bar{1}$	$Pna2_1$	$P2_1/n$	$P2_1/n$
Z	4	4	4	4
Radiation type	MoKα	MoKα	CuKα	CuKα
Absorption coefficient, μ/mm^{-1}	5.631	3.819	6.487	6.613
No. of reflections measured	35979	75112	18321	8203
No. of independent reflections	14346	13030	3484	8203
R$_{int}$	0.0338	0.0260	0.038	0.000
Final R1 values (I > 2σ(I))	0.0281	0.0177	0.0231	0.0378
Final wR(F^2) values (I > 2σ(I))	0.0504	0.0360	0.0559	0.0757
Final R1 values (all data)	0.0455	0.0203	0.0259	0.0483
Final wR(F^2) values (all data)	0.0551	0.0369	0.0593	0.0813
Goodness of fit on F^2	1.033	1.103	0.9420	0.9133
Flack x determined using quotients [(I+)-(I-)]/[(I+)+(I-)]		-0.0194(15)		

Table S2: Crystallographic parameters of the complexes **17** and **19**.

	17	**19**·2 *n*-hexane
CCDC number	1983664	1983666
Chemical formula	$C_{23}H_{18}N_3PO_5$ Mo	$C_{34}H_{18}N_6P_2O_4Br_6$ Mo
Formula mass	543.31	1211.88
Crystal system	monoclinic	triclinic
a/Å	10.4126(3)	10.7277(6)
b/Å	22.0156(5)	11.7959(5)
c/Å	10.8107(3)	19.1179(7)
α/°	90	79.702(3)
β/°	109.128(3)	84.994(4)
γ/°	90	65.607(5)
Unit cell volume/$Å^3$	2341.4(1)	2167.5(2)
Temperature/K	130	130
Space group	$P2_1/n$	$P\bar{1}$
Z	4	2
Radiation type	MoKα	MoKα
Absorption coefficient, μ/mm^{-1}	0.667	5.949
No. of reflections measured	20609	27582
No. of independent reflections	7736	14088
R_{int}	0.0270	0.0375
Final R1 values (I > 2σ(I))	0.0332	0.0449
Final wR(F^2) values (I > 2σ(I))	0.0649	0.0961
Final R1 values (all data)	0.0463	0.0788
Final wR(F^2) values (all data)	0.0698	0.1064
Goodness of fit on F^2	1.028	1.032
Flack x determined using quotients [(I+)-(I-)]/[(I+)+(I-)]		

6.) Computational Details

Table S3: Different functionals for the determination of the symmetric carbonyl stretching frequency in [Ni(CO)$_3$(P^{t}Bu$_3$)].

Functional	νCO [cm^{-1}]
TPSS	**2042**
BP86	2029
revPBE	2018
M06	2157